

## Temperature dependence of hyperfine interactions and of anisotropy of recoil-free fraction: A Mössbauer study of the 93.3-keV resonance of $^{67}\text{Zn}$ in single crystals of zinc metal

W. Potzel, W. Adlassnig, Ulrike Närger, Th. Obenhuber, K. Riski,\* and G. M. Kalvius

*Physik-Department E15, Technische Universität München, D-8046 Garching, Federal Republic of Germany*

(Received 30 April 1984)

The temperature dependence of the anisotropy of the Lamb-Mössbauer factor (LMF) and of the hyperfine interactions in Zn metal single crystals has been investigated in the temperature range between 4.2 and 47 K using the sharply-defined 93.3-keV transition in  $^{67}\text{Zn}$ . The anisotropy of the LMF is very pronounced and changes markedly with temperature: The mean-square atomic displacements perpendicular to and along the  $c$  axis were found to be  $\langle x^2 \rangle_{\perp} = (0.00226 \pm 0.00005) \text{ \AA}^2$  and  $\langle x^2 \rangle_{\parallel} = (0.0037 \pm 0.0005) \text{ \AA}^2$  at 4.2 K and  $\langle x^2 \rangle_{\perp} = (0.00270 \pm 0.00007) \text{ \AA}^2$  and  $\langle x^2 \rangle_{\parallel} = (0.0061 \pm 0.0016) \text{ \AA}^2$  at 47 K. The quadrupole interaction is  $e^2qQ/h = (12.30 \pm 0.08) \text{ MHz}$  independent of temperature. At 47 K the center shift has changed by  $(4.6 \pm 0.3) \mu\text{m/s}$  compared to its value at 4.2 K due to second-order Doppler shift (SOD). The results on the LMF and SOD can be very well described by an extended Debye model characterized by the two Debye temperatures  $\Theta_{\perp} = (242 \pm 10) \text{ K}$  and  $\Theta_{\parallel} = (149 \pm 20) \text{ K}$ . The data are also compared with a recent modified axially symmetric model calculation, where a recursion method was applied. The quadrupole data extend earlier measurements obtained by the time differential perturbed angular distribution method. Together with those they show that the  $T^{3/2}$  law is not valid at low temperature.

### I. INTRODUCTION

Even in the early days of Mössbauer spectroscopy the 93.3-keV transition in  $^{67}\text{Zn}$  was recognized<sup>1</sup> as offering extremely high resolution for the determination of small changes in energy. This exceptionally high sensitivity has been primarily used for precision measurements of hyperfine interactions. Magnetic fields of only 0.01 T produce a completely resolved nuclear Zeeman pattern.<sup>2</sup> The quadrupole interaction of the spin- $\frac{5}{2}$  ground state of  $^{67}\text{Zn}$  has been thoroughly investigated in ZnO (Refs. 3–7) and in zinc metal<sup>7–10</sup> at 4.2 K. Large isomer shifts have been observed for zinc chalcogenides,<sup>11,12</sup> for  $\text{ZnF}_2$ ,<sup>12</sup> and recently also for various Cu-Zn alloys (brass).<sup>13</sup>

The high energy resolution was further used to study relativistic effects, the second-order Doppler shift,<sup>5,12</sup> and the shift of 93.3-keV photons in the gravitational field of the Earth.<sup>14,15</sup>

Only very recently it has been shown by a determination of the anisotropy of the Lamb-Mössbauer factor (LMF) in zinc-metal single crystals at 4.2 K that this unusual Mössbauer resonance is also a most sensitive tool for studying lattice dynamics.<sup>16</sup>

Zinc metal, which crystallizes in a hexagonal structure, is of particular interest since the anisotropy found<sup>16</sup> for the LMF and the mean-square atomic displacements  $\langle x^2 \rangle_{\parallel}$  and  $\langle x^2 \rangle_{\perp}$ , parallel and perpendicular to the  $c$  axis, respectively, is exceptionally large. This is reflected by the unusually high  $c/a$  ratio ( $c/a = 1.861$ ) (Ref. 17) and furthermore by the rather complex phonon frequency distribution.<sup>18</sup>

Values for mean-square atomic displacements have been deduced from thermodynamic and x-ray and neutron scattering studies performed above 85 K (Ref. 19) and

from numerical lattice calculations.<sup>20</sup>

In the present paper we report on an extension of our previous Mössbauer resonance experiments<sup>16</sup> performed with single crystals of Zn metal. It was our aim to derive mean-square atomic displacements  $\langle x^2 \rangle_{\parallel}$  and  $\langle x^2 \rangle_{\perp}$  and the second-order Doppler shift (SOD) in the temperature range between 4 and 50 K. Much higher temperatures cannot be used because of the small recoil-free fraction of the  $^{67}\text{Zn}$  resonance in Zn metal. We describe the results on the LMF and SOD by an extended Debye model and compare our data with predictions of the modified axially symmetric model<sup>21,18</sup> (MAS), in particular with a recent calculation where a recursion method was applied to the MAS model.<sup>20</sup> The temperature dependence of the electric field gradient (EFG) in Zn metal is discussed in light of modern theories.<sup>22</sup>

### II. EXPERIMENTAL DETAILS

#### A. Doppler velocity spectrometer

Measurements were performed in a standard transmission geometry. The Doppler velocities were generated by a piezoelectric quartz spectrometer whose basic design has been described elsewhere<sup>12</sup> but which contains some modifications for changing the temperature of the source. Figure 1 depicts the piezoelectric drive system. Three quartz crystals (only one is shown in the upper part of Fig. 1) were arranged in the shape of a regular triangle (see lower part of Fig. 1). The quartz crystals were  $X$  cut and were 100 mm long ( $y$  direction), 10 mm wide ( $z$  direction), and 3 mm thick ( $x$  direction). A sinusoidal voltage was applied to the  $(y,z)$  faces which were gold plated. The three crystals were electrically connected in parallel. The

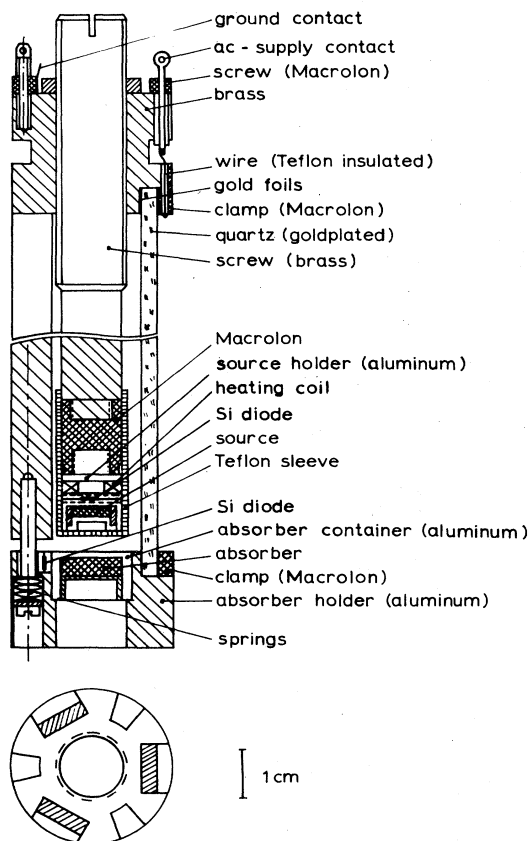


FIG. 1. Design of the piezoelectric Mössbauer drive. The lower part of the figure displays the geometrical arrangement of the three quartz crystals. The source can be heated to elevated temperatures.

piezoelectric elongations and contractions of interest occur in the  $y$  direction.<sup>12</sup> With sinusoidal voltage profiles, velocities up to  $\pm 300 \mu\text{m/s}$  have been scanned. The system has also been used for observing the natural width of  $^{67}\text{Zn}$  resonance lines.<sup>23</sup>

The temperature of the source could be increased by a small heating coil wrapped around the aluminum source holder. The temperature was measured by a calibrated Si diode of N-446 type placed immediately above the source single crystal and maintained at the desired value by a controller. To avoid excess heat flow, the source holder was thermally insulated from the brass screw by a macrolon connector and shielded by a teflon sleeve. A second N-446 Si diode which was located at the aluminum absorber holder monitored the temperature of the absorber.

The drive was suspended by soft springs inside a sealed stainless-steel container filled with He gas, the pressure of which could be adjusted in order to reach higher temperatures of the source. The container was then inserted into a liquid-He cryostat. This system worked very reliably. Even at a source temperature of 60 K, the absorber stayed below 15 K.

## B. Source preparation

The  $^{67}\text{Ga}$  ( $T_{1/2} = 78 \text{ h}$ ) activity was produced *in situ* by bombardment of Zn-metal single crystals by 14-MeV deuterons at the cyclotron of the Kernforschungszentrum Karlsruhe. The Zn single crystals with the natural abundance of  $^{67}\text{Zn}$  were disks of 7-mm diameter and of 1-mm thickness. They were cut in such a way that Mössbauer spectra could be recorded with the  $c$  axis at  $90^\circ$ ,  $75^\circ$ ,  $60^\circ$ , and  $55^\circ$  with respect to the direction of observation of the gamma rays. After irradiation the samples were annealed in an argon atmosphere at 420 K for 90 min and thereafter slowly cooled ( $25 \text{ K/hr}$ ) to room temperature. Measurements were started about 1.5 days after the end of the deuteron bombardment. Usually sources were good for about 10 days of counting. At elevated temperatures the absorption strength was so small that several sources were needed in order to obtain sufficient statistical accuracy (see Figs. 4 and 5). For the same reason only the  $90^\circ$  and  $75^\circ$  orientations were investigated in these cases.

## C. Characterization of $\beta'$ -brass absorber

The absorber consisted of a Cu-Zn alloy with 49.2 at. % Zn ( $\beta'$  brass), enriched to 91.9% in  $^{67}\text{Zn}$ . It provides a rather narrow (full width at half maximum =  $2.06 \pm 0.08 \mu\text{m/s}$ ) single absorption line with a center shift of  $-(6.15 \pm 0.02) \mu\text{m/s}$  with respect to a  $^{67}\text{GaCu}$  source.<sup>13</sup> The absorption spectrum is displayed in Fig. 2. We have performed additional experiments using a  $^{67}\text{GaCu}$  source and an enriched  $^{67}\text{ZnO}$  absorber. From the known<sup>23</sup> effective Debye temperature for ZnO ( $\Theta_D^{\text{ZnO}} = 309 \text{ K}$ ) we deduce a recoil-free fraction of  $\sim 1\%$  for this Cu-Zn alloy. This value thus depends only on  $\Theta_D^{\text{ZnO}}$ , but not on uncertainties of the recoil-free fraction of the  $^{67}\text{GaCu}$  source. Details will be published elsewhere.<sup>24</sup>

## D. Velocity calibration and nuclear pulse counting

The spectrometer was calibrated using the known quadrupole splittings in  $^{67}\text{Zn}$  metal<sup>7,8</sup> and in  $^{67}\text{ZnO}$ ,<sup>6,7</sup> which have previously been measured absolutely by frequency-

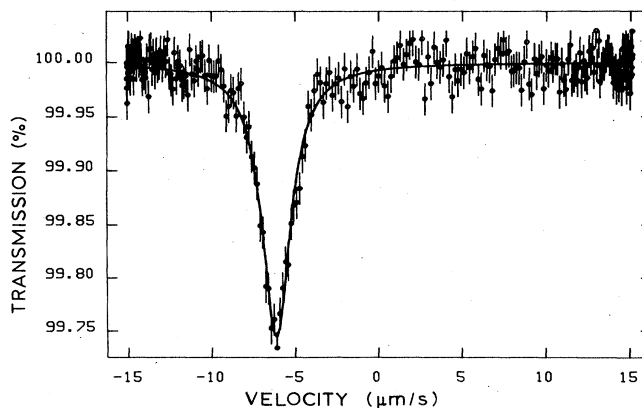


FIG. 2. Mössbauer absorption spectrum of a  $\beta'$ -brass absorber, enriched in  $^{67}\text{Zn}$ . The source is  $^{67}\text{GaCu}$ . Source and absorber at 4.2 K.

modulation techniques. Recording the spectra of both samples also provides a critical test for the linearity of the Doppler sweep.

The gamma rays were detected by an intrinsic Ge diode of 10-mm thickness and 40-mm diameter coupled to a fast preamplifier. In order to achieve high counting speeds and simultaneously good energy resolution a fast double differentiating main amplifier<sup>25</sup> was especially developed for these experiments. This amplifier, which allows shaping times as small as 50 ns to avoid pile-up effects, was used together with a 10-MHz single-channel analyzer.<sup>26</sup> The signal-to-background ratio  $S/(S+B)$  was determined several times a day by recording pulse-height spectra via a fast analog-to-digital converter<sup>26</sup> (ADC) in a separate multichannel analyzer. Typically,

$S/(S+B)$  values of 50% were obtained at count rates up to  $200\,000\text{ s}^{-1}$  in the 93.3-keV window. Data were collected in time mode into a 1024-channel analyzer featuring short ( $\sim 100\text{ ns}$ ) channel dwell times with virtually zero dead time.<sup>12</sup>

### III. RESULTS

#### A. Lamb-Mössbauer factor

Figure 3 displays Mössbauer absorption spectra recorded at 4.2 K for three orientations of the Zn single crystal. Figures 4 and 5 show spectra obtained at 20.8 and 47 K, respectively, for orientations of  $\vartheta=90^\circ$  and  $75^\circ$  of the  $c$  axis with respect to the direction of observation of the 93.3-keV gamma rays. The absorber was  $\beta'$  brass. The spectra were fitted by a superposition of three independent Lorentzian lines. The results are summarized in Table I. The values for the line positions obtained at 4.2 K for all four orientations of the zinc single crystals agree very well with the results of our earlier experiment on zinc-metal powder where we applied the frequency-modulation method,<sup>7,8</sup> and also with NMR measurements.<sup>27,28</sup>

The Lamb-Mössbauer factor and the mean-square atomic displacements are derived from the total area under the three absorption lines after correction for non-resonant background radiation has been applied. If  $\vec{k}$  is the wave vector of the gamma radiation and  $\vartheta$  denotes the angle between the  $c$  axis and  $\vec{k}$  (the direction of observation of gamma rays),  $f(\vartheta)$  is given by

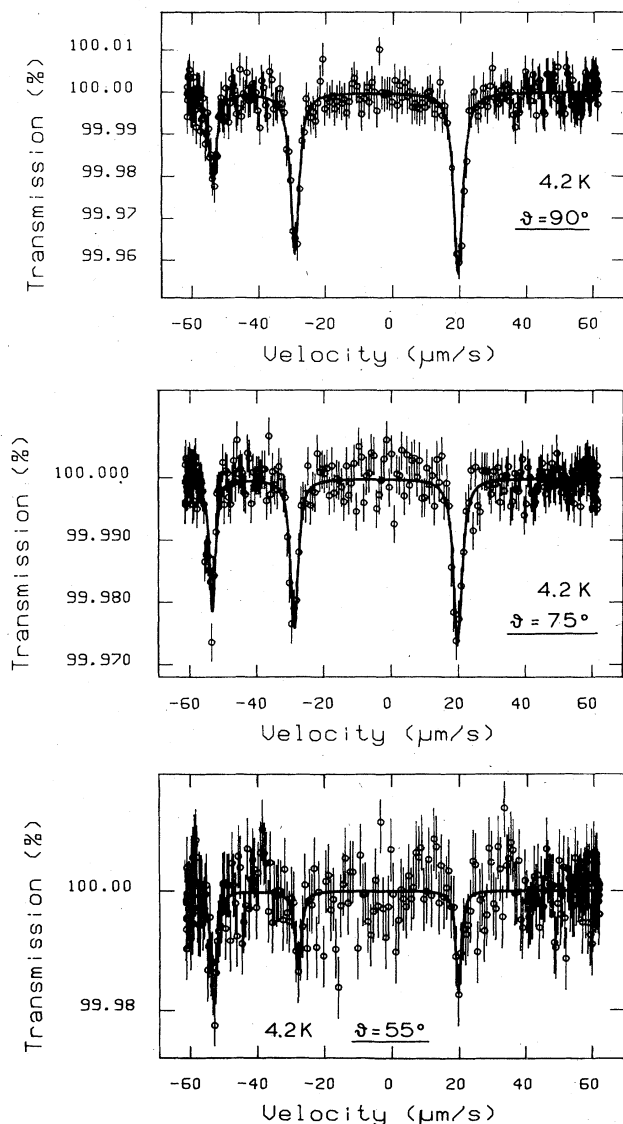


FIG. 3. Mössbauer absorption spectra obtained at 4.2 K. Sources are  $^{67}\text{GaZn}$  single crystals with three different orientations  $\vartheta$  of the  $c$  axis with respect to the direction of observation of the 93.3-keV gamma rays. The absorber is  $\beta'$  brass.

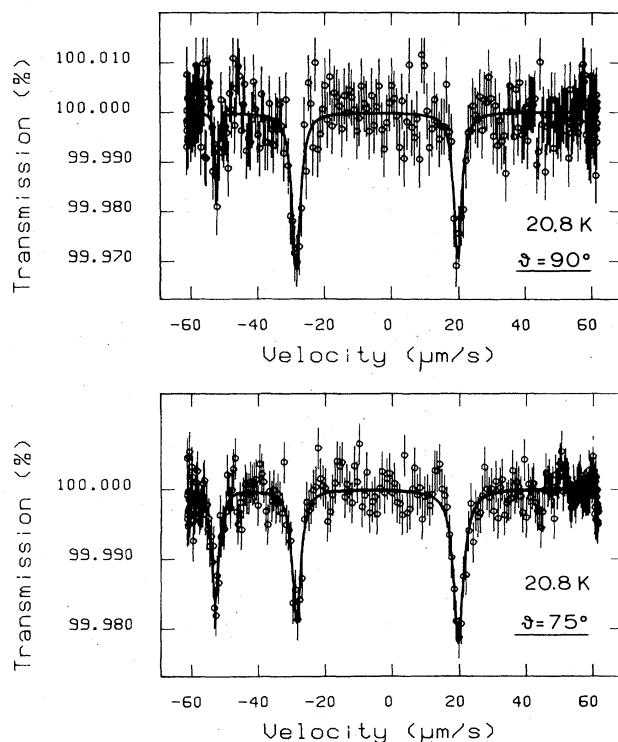


FIG. 4. Mössbauer absorption spectra obtained at 20.8 K for two orientations  $\vartheta$  of the  $^{67}\text{GaZn}$  single-crystal source. The absorber is  $\beta'$  brass at 4.2 K.

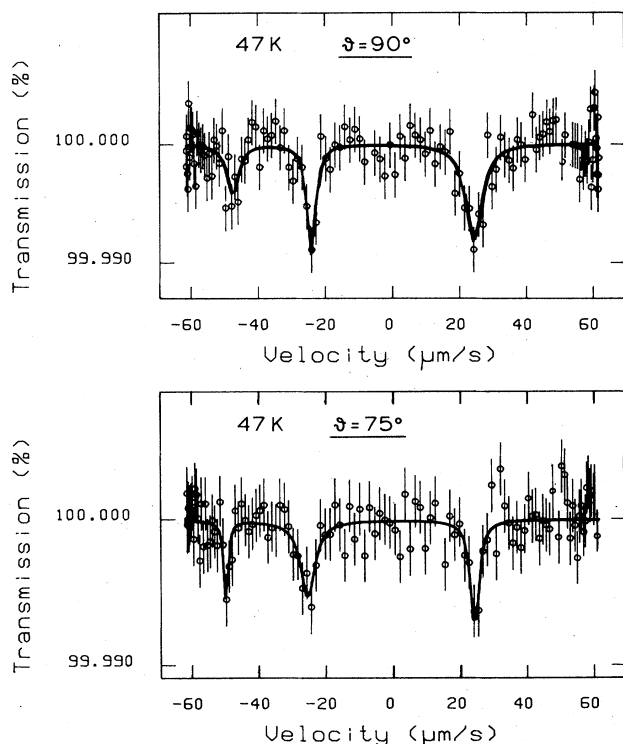


FIG. 5. Mössbauer absorption spectra taken at 47 K for two orientations  $\vartheta$  of the  $^{67}\text{GaZn}$  single-crystal source. The absorber is  $\beta'$  brass at 4.2 K.

$$f(\vartheta) = \exp\{-\bar{k}^2[\langle x^2 \rangle_{\perp} + (\langle x^2 \rangle_{\parallel} - \langle x^2 \rangle_{\perp})\cos^2\vartheta]\}.$$

From this equation a linear relation is expected between  $\ln[f(\vartheta)]$  and  $\cos^2\vartheta$  at each temperature investigated. As an example, Fig. 6 displays such a plot of our data obtained at 4.2 K. The values derived for the mean-square atomic displacements perpendicular and along the  $c$  axis of Zn metal are given in Table II together with the corresponding LM factors  $f_{\perp}$  and  $f_{\parallel}$ . The errors given include the statistical errors of the measurements and a 10% uncertainty in the determination of the signal-to-noise ratio in the gamma-ray spectrum. It is the evaluation of the latter which seriously limits the accuracy of  $\langle x^2 \rangle$  at 4.2 K.

### B. Quadrupole interaction

Due to the quadrupole splitting of the  $\frac{5}{2}$  ground state the Mössbauer spectra consist of three line patterns at all orientations investigated here. Only the relative intensities of the lines are changing with orientation at a fixed temperature (see Figs. 3–5). The line separations are a direct measure of the main component of the quadrupole tensor and the asymmetry parameter  $\eta$ .<sup>7,8</sup> As can be seen from Table I and Fig. 7 there is no change at all of the quadrupole interaction with temperature. We get  $e^2qQ/h = (12.30 \pm 0.08)$  MHz at 4.2 K and for the ratio  $e^2qQ(47 \text{ K})/e^2qQ(4.2 \text{ K}) = 1.002 \pm 0.007$ . The asymmetry parameter is found to be  $\eta = 0$  at all three temperatures.

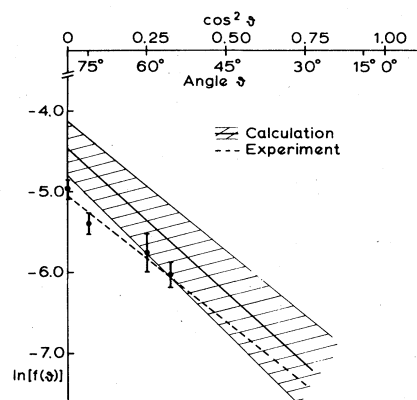


FIG. 6. Logarithm of Lamb-Mössbauer factor plotted versus  $\cos^2\vartheta$ . The dashed line is a least-squares fit to the data points obtained at 4.2 K, the shaded area represents results of calculations of Refs. 19 and 20.

### C. Center shift

A center shift of  $(4.6 \pm 0.3)$   $\mu\text{m/s}$  is found between 4.2 and 47 K (see Table I). This shift is mainly due to the second-order Doppler shift,<sup>29</sup> the isomer shift staying constant in this temperature regime (see below).

## IV. DISCUSSION

### A. Lamb-Mössbauer factor

As demonstrated in Table II, the anisotropy of the LMF is very large indeed: The ratio ( $f_{\perp}/f_{\parallel}$ ) is about 23 at 4.2 K and rises to  $\sim 2100$  at 47 K. This fact prevents measurements at crystal orientations much below  $\vartheta = 60^\circ$  and  $75^\circ$  at 4.2 and 50 K, respectively.

The simple Debye model clearly is not sufficient to characterize the phonon spectrum of such a highly anisotropic material. We will discuss our results in light of an extended Debye model (EDM). The temperature variations of  $f_{\perp}$  and  $f_{\parallel}$  are well described by effective Debye temperatures of  $\Theta_{\perp} = (242 \pm 10)$  K and  $\Theta_{\parallel} = (149 \pm 20)$  K, respectively. Thus in our EDM the phonon spectrum<sup>18</sup> is approximated by two Debye-type distributions characterized by  $\Theta_{\perp}$  and  $\Theta_{\parallel}$  as indicated in Fig. 8, the relative

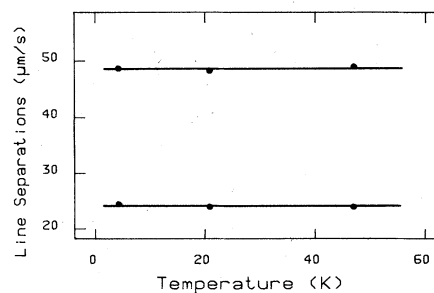


FIG. 7. Separation between absorption lines obtained at various temperatures. There is no detectable change of the quadrupole interaction within an error of  $7 \times 10^{-3}$ .

TABLE I. Summary of measured Mössbauer parameters for different orientations of Zn-metal single crystals at 4.2, 20.8, and 47 K, respectively. Only statistical errors are quoted.

Orientation of single crystal	Position ( $\mu\text{m/s}$ )	Width ( $\mu\text{m/s}$ )	Area ( $\mu\text{m/s}\%$ )	Temperature (K)
$\vartheta = 90^\circ$	$-53.5 \pm 0.2$	$2.7 \pm 0.4$	$0.057 \pm 0.006$	4.2
	$-29.0 \pm 0.1$	$2.9 \pm 0.3$	$0.113 \pm 0.008$	
	$19.7 \pm 0.1$	$3.1 \pm 0.3$	$0.133 \pm 0.009$	
$\vartheta = 75^\circ$	$-53.5 \pm 0.1$	$2.2 \pm 0.3$	$0.047 \pm 0.004$	4.2
	$-29.1 \pm 0.2$	$2.5 \pm 0.4$	$0.063 \pm 0.007$	
	$19.6 \pm 0.2$	$2.9 \pm 0.4$	$0.079 \pm 0.007$	
$\vartheta = 60^\circ$	$-53.0 \pm 0.3$	$2.5 \pm 0.9$	$0.055 \pm 0.014$	4.2
	$-27.7 \pm 0.9$	$3.0 \pm 2.5$	$0.031 \pm 0.020$	
	$19.9 \pm 0.5$	$3.5 \pm 1.6$	$0.067 \pm 0.022$	
$\vartheta = 55^\circ$	$-53.1 \pm 0.2$	$2.1 \pm 0.6$	$0.040 \pm 0.008$	4.2
	$-27.9 \pm 0.4$	$2.3 \pm 1.0$	$0.030 \pm 0.010$	
	$19.7 \pm 0.3$	$1.8 \pm 0.7$	$0.031 \pm 0.009$	
$\vartheta = 90^\circ$	$-52.4 \pm 0.2$	$1.0 \pm 0.4$	$0.019 \pm 0.006$	20.8
	$-28.6 \pm 0.2$	$2.9 \pm 0.5$	$0.096 \pm 0.012$	
	$19.7 \pm 0.2$	$2.8 \pm 0.5$	$0.084 \pm 0.012$	
$\vartheta = 75^\circ$	$-52.8 \pm 0.1$	$2.5 \pm 0.4$	$0.040 \pm 0.004$	20.8
	$-28.6 \pm 0.1$	$2.9 \pm 0.4$	$0.056 \pm 0.006$	
	$19.8 \pm 0.1$	$3.5 \pm 0.4$	$0.077 \pm 0.007$	
$\vartheta = 90^\circ$	$-47.7 \pm 0.6$	$3.9 \pm 1.9$	$0.018 \pm 0.007$	47
	$-24.2 \pm 0.3$	$2.8 \pm 1.1$	$0.028 \pm 0.007$	
	$23.9 \pm 0.5$	$5.3 \pm 1.5$	$0.046 \pm 0.010$	
$\vartheta = 75^\circ$	$-49.6 \pm 0.3$	$1.4 \pm 0.9$	$0.009 \pm 0.003$	47
	$-25.2 \pm 0.6$	$5.2 \pm 1.9$	$0.028 \pm 0.008$	
	$24.6 \pm 0.3$	$3.1 \pm 1.2$	$0.023 \pm 0.006$	

weight of the two distributions being 2:1. The relatively low value of  $\Theta_{\parallel}$  is caused by the large peak around 95 K in the phonon frequency distribution. This peak mainly originates from lattice vibrations parallel to the  $c$  axis. From such a situation, where  $\Theta_{\parallel}$  corresponds to a higher frequency than the position of this peak, one would expect a large temperature dependence of the effective Debye temperature  $\Theta^{sp}$  as determined by specific-heat measurements.<sup>30</sup> This is fully corroborated by experiments,<sup>31,32</sup>

where it was found that  $\Theta^{sp} = 203$  K at 20 K and rises to  $\Theta^{sp} = 307$  K at 4 K. In fact, the temperature variation of the specific heat is convincingly reproduced by the EMD, using slightly higher Debye temperatures ( $\Theta_{\perp} = 255$  K,  $\Theta_{\parallel} = 160$  K) although we found that a comparison with specific-heat data gives a rather broad range of temperatures for  $\Theta_{\perp}$  and  $\Theta_{\parallel}$  and therefore is not a critical test.

In Fig. 9 the mean-square atomic displacements are plotted versus temperature. The full lines represent fits by

TABLE II. Lamb-Mössbauer factors  $f_{\perp}$  and  $f_{\parallel}$ , perpendicular and along the  $c$  axis of Zn metal, respectively, and corresponding mean-square atomic displacements obtained at 4.2, 20.8, and 47 K. The errors quoted include the statistical errors and a 10% uncertainty in the determination of the signal-to-noise ratio in the gamma-ray spectrum.

Lamb-Mössbauer factors		Mean-square atomic displacements ( $\text{\AA}^2$ )		Temperature (K)
$f_{\perp}$	$f_{\parallel}$	$\langle x^2 \rangle_{\perp}$	$\langle x^2 \rangle_{\parallel}$	
$(6.4^{+0.8}_{-0.7}) \times 10^{-3}$	$(2.6^{+5.3}_{-1.8}) \times 10^{-4}$	$0.00226 \pm 0.00005$	$0.0037 \pm 0.0005$	4.2
$(4.8^{+1.1}_{-0.9}) \times 10^{-3}$	$(5.9^{+32}_{-4.8}) \times 10^{-4}$	$0.00239 \pm 0.00009$	$0.0033 \pm 0.0008$	20.8
$(2.4^{+0.9}_{-0.3}) \times 10^{-3}$	$(1.1^{+40}_{-1.0}) \times 10^{-6}$	$0.00270 \pm 0.00010$	$0.0061 \pm 0.0016$	47



damage caused by the 14-MeV deuterons is annealed to a very large extent.

(3) The signal-to-noise ratio may be overestimated due to pile-up effects at the high count rates used. Also this possibility is unlikely, since very fast electronic equipment was employed (see Sec. IID); in particular, a high-speed main amplifier allowing shaping times as short as 50 ns.<sup>25</sup>

In summary, our data on the LMF can best be represented by the extended Debye model characterized by two independent phonon density-of-states distributions with Debye temperatures  $\Theta_{\perp}$  and  $\Theta_{\parallel}$ , respectively. The consequences of this model for the second-order Doppler shift will be discussed now.

### B. Center shift

The experimentally observed temperature variation of the center shift  $C$  can be written<sup>36,37</sup>

$$\begin{aligned} (\partial C/\partial T)_P = & (\partial S_{\text{SOD}}/\partial T)_P + (\partial S/\partial T)_V \\ & + (\partial S/\partial \ln V)_T (\partial \ln V/\partial T)_P. \end{aligned}$$

The first term represents the second-order Doppler shift. The second term describes the explicit temperature dependence of the isomer shift  $S$  at constant volume due to changes of the electron density caused by the electron-phonon interaction upon the electronic states of the conduction electrons.<sup>38</sup> The third term accounts for the volume dependence of  $S$  caused by thermal expansion of the lattice. The last two terms are expected to change very little with temperature: Explicit temperature dependences of  $S$  have been found at higher temperatures for  $\beta$  tin,<sup>37</sup> for iron metal and other systems containing iron,<sup>39,40</sup> and for tantalum in various host metals.<sup>41</sup> In all cases, the electron density at the nucleus was found to increase with temperature by amounts corresponding to  $\sim 10^{-5}$  of an  $s$  electron in  $s$ -like valence-band states per degree. Using this number and the known value of  $\Delta \langle r^2 \rangle$  (Ref. 12) together with calculations of electron densities at the  $^{67}\text{Zn}$  nucleus<sup>42</sup>  $(\partial S/\partial T)_V$  can be estimated. The biggest change (worst case) is expected if one assumes that all conduction electrons are  $s$  electrons (they also have, of course,  $p$  character to a large extent). According to Ref. 42 the removal of two  $s$  electrons would decrease the  $s$  electron density at the nucleus by  $\sim 15a_0^{-3}$ . Thus  $\Delta S \sim 0.07 \mu\text{m/s}$  between 4.2 and 47 K and can be expected to be even smaller, since our measuring temperatures are low.

The lattice expansion is only  $\sim 1 \times 10^{-3}$  between 4.2 and 47 K.<sup>43-45</sup> Applying a simple scaling assumption for the change of the  $4s$  density  $\rho$ ,

$$\Delta \rho = -(\Delta V/V)\rho,$$

we estimate  $\Delta S \sim 0.1 \mu\text{m/s}$ , or only  $\sim 2\%$  of the center shift observed between 4.2 and 47 K. Again, this value can be expected to be even smaller.<sup>46</sup> Thus, to a very good approximation  $\Delta C = \Delta S_{\text{SOD}}$ .

Since the SOD is independent of orientation it can be characterized by an average Debye temperature in the simple Debye model. The fit to the SOD data gives a Debye temperature of  $\Theta_D^{\text{SOD}} = (202 \pm 8)$  K. This is in remarkable agreement with an average Debye temperature of

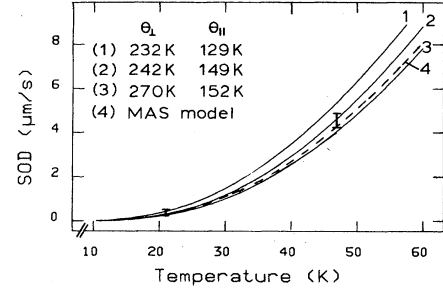


FIG. 10. Second-order Doppler shift at various temperatures. Curve (2) is obtained from extended Debye model of Fig. 8 and gives the best fit to the data points. Curve (4) is the result of MAS model calculations. All curves are normalized to zero shift at 0 K.

$\langle \Theta_D \rangle = (211 \pm 6)$  K as determined from the LMF's, averaged over all orientations in space.

Applying the extended Debye model with  $\Theta_{\perp} = 242$  K and  $\Theta_{\parallel} = 149$  K to the SOD we calculate  $\Delta S_{\text{SOD}} = 4.67 \mu\text{m/s}$  which is in excellent agreement with our experimental value of  $\Delta S_{\text{SOD}} = 4.6 \mu\text{m/s}$ . This is depicted in Fig. 10, where the center shift is plotted versus temperature. The prediction of the MAS model<sup>21,18</sup> is also shown in Fig. 10. On the scale of the figure and in the temperature range presented there is no difference if the root-sampling method<sup>18</sup> or the recursion method<sup>20</sup> is applied to the MAS.

Our values for the SOD are again somewhat larger than those predicted by the MAS model.<sup>20</sup> This is consistent with the systematic deviations discussed in Sec. IV A and is regarded as a further hint that cause (1) is responsible for the discrepancies. Clearly, the SOD weighing the phonon spectrum with  $\omega$  is much less sensitive to the lower frequency part than the LMF.

### C. Quadrupole interaction

As demonstrated in Table I and Fig. 7 the quadrupole interaction is independent of temperature between 4.2 and 47 K to a precision of  $7 \times 10^{-3}$ . This behavior can be described by a relation found empirically<sup>47,48</sup> in the high-temperature ( $T > 200$  K) regime:  $eq(T)/eq(0) = 1 - BT^{3/2}$  with  $B = (1.20 \pm 0.04) \times 10^{-5} \text{ K}^{-3/2}$  which gives a reduction at 47 K of only  $4 \times 10^{-3}$  being clearly within our limits of error. The problem, however, is that in light of other experiments and modern theories the  $T^{3/2}$  "law" should not be applicable in our temperature regime and therefore the agreement described above might just be fortuitous.

Using a screened potential of the ions in order to take into account the contribution of the conduction electrons the EFG can be written as<sup>49,50</sup>

$$eq(T) = (1 - \gamma_{\text{eff}}) eq_{\text{ion}}^{\text{sc}}(T) \exp\left[-\frac{4}{3} \vec{k}_F^2 \langle u^2 \rangle(T)\right],$$

where  $(1 - \gamma_{\text{eff}})$  is a Sternheimer-type enhancement factor which is due to the polarization of the screened ions and is assumed to be temperature independent. The influence of the lattice vibrations on the EFG is described by the Debye-Waller factor which contains the vector  $\vec{k}_F$  of the electrons at the Fermi surface. The term  $eq_{\text{ion}}^{\text{sc}}(T)$  is a lat-

tice sum over the screened ions<sup>50</sup> which depends on the temperature-dependent lattice constants and on  $\vec{k}_F$ , which changes only slightly with temperature because of volume expansion. The Debye-Waller factor always decreases with temperature. The product yields to a good approximation a  $(-T^{3/2})$  dependence<sup>49,50</sup> over a wide temperature range, although isotropic thermal motion is assumed (as in cubic metals). This condition was relaxed in an elaborate first-principles calculation of electronic [ $q_{el}(T)$ ] and lattice contributions [ $q_{latt}(T)$ ] to the EFG in Zn and Cd.<sup>22</sup> It was found that by far the major contribution to the temperature variation of  $q_{el}(T)$  arises from the isotropic phonons, whereas the variation of  $q_{latt}(T)$  is determined by the anharmonic and anisotropic aspects of the phonons, the anharmonic lattice contribution being substantially smaller than the anharmonic one. Although the temperature range investigated in Ref. 22 does not cover low temperatures it seems clear that all contributions cause a decrease of the EFG with increasing temperature except the anisotropic lattice contribution which is slowly rising. It appears doubtful, however, that the anisotropic part being the smallest is able to compensate all others in the temperature range between 4.2 and 50 K, a necessary condition to explain our experimental results.

A semiclassical so-called "naive model"<sup>51</sup> gave reasonable results at higher temperatures but is not in agreement with experiments in the low-temperature regime.

In a recent attempt<sup>52,53</sup> the EFG and its temperature dependence were calculated within the framework of the phonon theory of metals. This model leads to a  $(T/\Theta_D)^4$  dependence of the EFG at low temperatures and predicts a decrease of the EFG in Zn metal of at least 1.3% at 47 K, which is too large to fit our data. In addition, the EFG at <sup>67</sup>Zn in Zn metal as determined by the time differential perturbed angular distribution (TDPAD) method seems to remain constant below  $\sim 170$  K (Ref. 47) and the EFG at Cd in Zn was found<sup>54</sup> to decrease only above  $\sim 150$  K, although in such an impurity system there always remains the question of impurity-host interactions.

It is obvious that our understanding of electric field gradients and their temperature dependence is poor. The experimental results call for considerable refinements in the theoretical calculations. In particular, experi-

ments<sup>13,24</sup> performed in this laboratory on the Cu-Zn alloy system (brass) suggest that  $d$  electrons—although energetically deep below the Fermi level<sup>55</sup>—might play an important role for hyperfine interactions. Thus the examination of the contribution to the EFG from bands associated with the  $d$  electrons, which have been treated as core electrons until now,<sup>22</sup> is most desirable.

## V. SUMMARY

The anisotropy of the mean-square atomic displacements has been determined for Zn metal between 4.2 and 47 K. The corresponding  $f$  factors perpendicular and parallel to the  $c$  axis vary by a factor of 2100 at the highest temperature investigated. This enormous anisotropy as well as the second-order Doppler shift can be impressively well described by a Debye distribution characterized by two Debye temperatures  $\Theta_{\perp}$  and  $\Theta_{\parallel}$ , respectively (extended Debye model). As compared to the MAS model the experimental data require a considerably larger phonon density at low frequencies. It is suggested that the extended Debye model gives accurate predictions also for other highly anisotropic cases, e.g., nearly two-dimensional systems.

The temperature variation of the electric-field gradient in Zn metal is still poorly understood from a theoretical point of view. Here a possible contribution from  $d$ -band electrons has to be checked.

Our measurements demonstrate that the <sup>67</sup>Zn Mössbauer resonance—famous for its extremely high energy resolution—is also a most sensitive tool for studying lattice dynamical effects.

## ACKNOWLEDGMENTS

We would like to thank the cyclotron crew of the Kernforschungszentrum Karlsruhe, especially Dr. H. Schweickert, K. Assmus, and W. Maier, for the numerous source irradiations. We are also grateful to N. Schultes, Dr. F. Pröbst, and M. Zelger for computational assistance. This work was supported by the Bundesministerium für Forschung und Technologie and by funds of the Kernforschungszentrum Karlsruhe.

\*On leave from Helsinki University of Technology, Department of Technical Physics, Finland.

<sup>1</sup>R. V. Pound and G. A. Rebka, Jr., Phys. Rev. Lett. 3, 439 (1959); 4, 397 (1960).

<sup>2</sup>G. J. Perlow, L. E. Campbell, L. E. Conroy, and W. Potzel, Phys. Rev. B 7, 4044 (1973).

<sup>3</sup>V. P. Alfimenkov *et al.*, J. Exptl. Theoret. Phys. (U.S.S.R.) 42, 1029 (1962) [Sov. Phys.—JETP 15, 713 (1962)].

<sup>4</sup>H. de Waard and G. J. Perlow, Phys. Rev. Lett. 24, 566 (1970).

<sup>5</sup>A. I. Beskrovny, N. A. Lebedev, and Yu. M. Ostanevich, JINR report, Dubna, 1971 (in Russian) (unpublished).

<sup>6</sup>G. J. Perlow, W. Potzel, R. M. Kash, and H. de Waard, J. Phys. (Paris) 35, C6-197 (1974).

<sup>7</sup>W. Potzel, Th. Obenhuber, A. Forster, and G. M. Kalvius, Hyperfine Interact. 12, 135 (1982).

<sup>8</sup>Th. Obenhuber, A. Forster, W. Potzel, and G. M. Kalvius, Nucl. Instrum. Methods 214, 361 (1983).

<sup>9</sup>W. T. Vetterling and R. V. Pound, *Workshop on New Directions in Mössbauer Spectroscopy (Argonne, 1977)*, proceedings of the Workshop on New Directions in Mössbauer Spectroscopy, edited by G. J. Perlow (AIP, New York, 1977).

<sup>10</sup>W. Potzel, A. Forster, and G. M. Kalvius, Phys. Lett. 67A, 421 (1978); and J. Phys. (Paris) 40, C2-29 (1979).

<sup>11</sup>D. Griesinger, R. V. Pound, and W. Vetterling, Phys. Rev. B 15, 3291 (1977).

<sup>12</sup>A. Forster, W. Potzel, and G. M. Kalvius, Z. Phys. B 37, 209

- (1980).
- <sup>13</sup>U. Narger, J. Zankert, W. Potzel, Th. Obenhuber, A. Forster, and G. M. Kalvius, *Hyperfine Interact.* **15/16**, 777 (1983).
- <sup>14</sup>T. Katila and K. Riski, *Phys. Lett.* **83A**, 51 (1981).
- <sup>15</sup>T. Katila and K. Riski, *Hyperfine Interact.* **13**, 119 (1983).
- <sup>16</sup>W. Potzel, U. Narger, Th. Obenhuber, J. Zankert, W. Adlassnig, and G. M. Kalvius, *Phys. Lett.* **98A**, 295 (1983).
- <sup>17</sup>C. Kittel, *Introduction to Solid State Physics*, 5th ed. (Wiley, New York, 1976), p. 24.
- <sup>18</sup>L. J. Raubenheimer and G. Gilat, *Phys. Rev.* **157**, 586 (1967).
- <sup>19</sup>T. H. K. Barron and R. W. Munn, *Acta Crystallogr.* **22**, 170 (1967), and references therein.
- <sup>20</sup>W. T. Vetterling and D. Candela, *Phys. Rev. B* **27**, 5394 (1983).
- <sup>21</sup>R. E. DeWames, T. Wolfram, and G. W. Lehman, *Phys. Rev.* **138**, A717 (1965).
- <sup>22</sup>M. D. Thompson, P. C. Pattnaik, and T. P. Das, *Phys. Rev. B* **18**, 5402 (1978).
- <sup>23</sup>W. Potzel, A. Forster, and G. M. Kalvius, *J. Phys. (Paris)* **37**, C6-691 (1976).
- <sup>24</sup>U. Narger, J. Zankert, W. Potzel, and G. M. Kalvius (unpublished).
- <sup>25</sup>W. Potzel and N. Halder, *Nucl. Instrum. Methods* (to be published).
- <sup>26</sup>Instrument manufactured by Halder Elektronik GmbH, Hohenbreitenweg 9, D-8110 Seehausen, W. Germany.
- <sup>27</sup>H. Herberg, J. Abart, and J. Voithlander, *Z. Naturforsch.* **34a**, 1029 (1979).
- <sup>28</sup>J. Abart, E. Palangi, W. Socher, and J. Voithlander, *J. Chem. Phys.* **78**, 5468 (1983).
- <sup>29</sup>G. K. Shenoy, F. E. Wagner, and G. M. Kalvius, in *Mossbauer Isomer Shifts*, edited by G. K. Shenoy and F. E. Wagner (North-Holland, Amsterdam, 1978), p. 101.
- <sup>30</sup>G. Leibfried, in *Handbuch der Physik*, edited by S. Flugge (Springer, Berlin, 1955), Vol. VII, part 1.
- <sup>31</sup>D. L. Martin, *Phys. Rev.* **167**, 640 (1968).
- <sup>32</sup>W. Eichenauer and M. Schulze, *Z. Naturforsch.* **14a**, 28 (1959).
- <sup>33</sup>E. O. Wollan and G. G. Harvey, *Phys. Rev.* **51**, 1054 (1937).
- <sup>34</sup>G. E. M. Jauncey and W. A. Bruce, *Phys. Rev.* **51**, 1067 (1937).
- <sup>35</sup>Finite solid-angle effects due to our transmission geometry were taken into account by a numerical integration routine.
- <sup>36</sup>R. V. Pound, G. B. Benedek, and R. Drever, *Phys. Rev. Lett.* **7**, 405 (1961).
- <sup>37</sup>G. M. Rothberg, S. Guimard, and N. Benczer-Koller, *Phys. Rev. B* **1**, 136 (1970).
- <sup>38</sup>R. V. Kasowski and L. M. Falicov, *Phys. Rev. Lett.* **22**, 1001 (1969).
- <sup>39</sup>R. M. Housley and F. Hess, *Phys. Rev.* **164**, 340 (1967).
- <sup>40</sup>D. L. Williamson, in *Mossbauer Isomer Shifts*, Ref. 29.
- <sup>41</sup>G. Kaindl, D. Salomon, and G. Wortmann, in *Mossbauer Isomer Shifts*, Ref. 29.
- <sup>42</sup>I. M. Band and V. I. Fomichev, *At. Data Nucl. Data Tables* **23**, 296 (1979).
- <sup>43</sup>R. W. Meyerhoff and J. F. Smith, *J. Appl. Phys.* **33**, 219 (1962).
- <sup>44</sup>R. D. McCammon and G. K. White, *Philos. Mag.* **11** (114), 1125 (1965).
- <sup>45</sup>Y. S. Touloukian, R. K. Kirby, R. E. Taylor, and P. D. Desai, *Thermo-Physical Properties of Matter, The TPRC Data Series* (Plenum, New York, 1975), Vol. 12.
- <sup>46</sup>L. D. Roberts, D. O. Patterson, J. O. Thomson, and R. P. Levey, *Phys. Rev.* **179**, 656 (1969).
- <sup>47</sup>J. Christiansen, P. Heubes, R. Keitel, W. Klinger, W. Loeffler, W. Sandner, and W. Witthuhn, *Z. Phys. B* **24**, 177 (1976), see, in particular, Table 4.
- <sup>48</sup>P. Heubes, G. Hembel, H. Ingwersen, R. Keitel, W. Klinger, W. Loeffler, and W. Witthuhn, in *Proceedings of the International Conference on Hyperfine Interactions Studied in Nuclear Reactions and Decay*, edited by E. Karlsson and R. Wappling (University of Uppsala, Uppsala, Sweden, 1974), p. 208.
- <sup>49</sup>P. Jena, *Phys. Rev. Lett.* **36**, 418 (1976).
- <sup>50</sup>K. Nishiyama, F. Dimmling, Th. Kornrumpf, and D. Riegel, *Phys. Rev. Lett.* **37**, 357 (1976).
- <sup>51</sup>E. Bodenstedt and B. Perscheid, *Hyperfine Interact.* **5**, 291 (1978).
- <sup>52</sup>W. Engel, W. Klinger, and W. Witthuhn, *Hyperfine Interact.* **9**, 247 (1981), and references therein.
- <sup>53</sup>W. Engel, H. Fottinger, R. Reichle, and W. Witthuhn, *Hyperfine Interact.* **15/16**, 249 (1983).
- <sup>54</sup>R. Keitel, W. Engel, H. Fottinger, D. Forkel, M. Iwatschenko-Borho, F. Meyer, and W. Witthuhn, *Hyperfine Interact.* **15/16**, 425 (1983).
- <sup>55</sup>G. K. Wertheim, M. Campagna, and S. Hufner, *Phys. Condens. Matter* **18**, 133 (1974).